Cephalopod Retinal Development Shows Vertebrate-like Mechanisms of Neurogenesis

Francesca Napoli*, Christina M. Daly*, Stephanie Neal, Kyle J. McCulloch, Alexandra Zaloga, Alicia Liu, Kristen M. Koenig

*These authors contributed equally to this work

John Harvard Distinguished Science Fellowship Program, Harvard University, Cambridge, MA 02138 USA.

Department of Organismic and Evolutionary Biology, Harvard University, Cambridge, MA 02138 USA

Email: kmkoenig@fas.harvard.edu

Abstract

Neurogenesis, the regulation of cellular proliferation and differentiation in the developing nervous system, is the process that underlies the diversity of size and cell type found in animal nervous systems. Our understanding of how this process has evolved is limited because of the lack of high resolution data and live-imaging methods across species. The retina is a classic model for the study of neurogenesis in vertebrates and live-imaging of the retina has shown that during development, progenitor cells are organized in a pseudostratified neuroepithelium and nuclei migrate in coordination with the cell cycle along the apicobasal axis of the cell, a process called interkinetic nuclear migration. Eventually cells delaminate and differentiate within the boundaries of the epithelium. This process has been considered unique to vertebrates and thought to be important in maintaining organization during the development of a complex nervous system. Coleoid cephalopods, including squid, cuttlefish and octopus, have the largest nervous system of any invertebrate and convergently-evolved camera-type eyes, making them a compelling comparative system to vertebrates. Here we have pioneered live-imaging techniques to show that the squid, *Doryteuthis pealeii*, displays cellular mechanisms during cephalopod retinal neurogenesis that are hallmarks of vertebrate processes. We find that retinal progenitor cells in the squid undergo interkinetic nuclear migration until they exit the cell cycle, we identify retinal organization corresponding to progenitor, post-mitotic and differentiated cells, and we find that Notch signaling regulates this process. With cephalopods and vertebrates having diverged 550 million years ago, these results suggest that mechanisms thought to be unique to vertebrates may be common to highly proliferative neurogenic primordia contributing to a large nervous system.

Introduction

Coleoid cephalopods (e.g. squid, cuttlefish and octopus) are known for their charismatic behaviors and their large nervous system. One of the striking features of the cephalopod nervous system is their camera-type eyes, which are one of the most acute visual organs among animals (Gagnon et al., 2013; Packard, 1972). This complexity in cephalopods is independently evolved from similar features found in vertebrate species. Although vertebrates have been well studied, the developmental changes that underlie the evolution of large, complex nervous systems are not well understood. Observations in traditional model organisms show that diversity in nervous system size and functionality across animals is a product of diversity in process (Hartenstein & Stollewerk, 2015). We know that in some cases neurogenesis is highly regulated with invariant numbers of precursors with fixed lineages (i.e. *C. elegans*), and in others cell lineage is stochastic or plastic (i.e. the vertebrate retina) (Bertrand & Hobert, 2010; Zechner et al., 2020; Hartenstein & Stollewerk, 2015). In addition, live-imaging has changed our perspective on neurodifferentiation from a primarily genetic process, to a cell biological process, defined by orchestrated cell behaviors and tissue architecture. However, our *in vivo* understanding of neurogenesis has been limited to very few species. To better understand how changes in neurogenesis may contribute to the evolution of large and complex nervous systems, we sought to understand neurodifferentiation in the cephalopod. The visual system has proven to be a powerful context to understand fundamental aspects of neural development in vertebrates and *Drosophila* and therefore we have chosen to focus our investigations on retinal differentiation in the squid *Doryteuthis pealeii.*

The adult cephalopod retina is composed of two layers divided by the basal membrane (Figure 1A). Photoreceptor cell bodies are found posterior to the basal membrane and support cells are found anterior. The photoreceptor cells extend projections to the anterior of the retina to form the outer segment layer, and extend axons out the posterior retina to synapse directly on the optic lobe (Yamamoto et al., 1965; Young, 1974). During development, photoreceptor cell bodies are first identified behind the basal membrane at Arnold embryonic stage 27, and these cells no longer incorporate Brdu (Arnold, 1965; Koenig et al., 2016). This is the earliest evidence of differentiation in the retina. The support cells in the anterior of the retina, also extend processes into the outer segment (Yamamoto et al., 1965). Although the eye at hatching is functional, the support cells continue to incorporate BrdU (Koenig et al., 2016). The animal continues to grow post-hatching and support cell proliferation may be a long term retinal stem cell population.

Previous observations from fixed tissue suggested that the cephalopod retinal primordia is a pseudostratified epithelium, which is unusual for an invertebrate neurogenic tissue (Koenig

et al, 2016; (Koenig & Gross, 2020)) (Figure 1A). This type of neuroepithelium is characteristic of central nervous system development in vertebrates, including the retina (Taverna et al., 2014). A pseudostratified epithelium is a monolayer composed of elongated cells with nuclei distributed along the apicobasal axis. Cells in pseudostratified epithelia undergo nuclear movement correlated with the cell cycle called interkinetic nuclear migration (Norden, 2017). This migration is required for proper differentiation and organization in the developing vertebrate nervous system (Strzyz et al., 2016). During nuclear migration, mitosis occurs on the apical surface and in vertebrates this corresponds to the posterior side of the developing retina (Baye & Link, 2008) (Figure 1A). In the cephalopod, fixed data suggests that mitosis occurs on the anterior side of the developing retina, inverted relative to vertebrates (Koenig et al., 2016) (Figure 1A). These observations lead us to ask whether cephalopod retinal progenitor cells undergo interkinetic nuclear migration and how cells differentiate within this epithelium.

Results

Cell cycle in the developing squid retina

Previous work in the squid retina showed that at stage 23, a 3 hour Brdu pulse showed incorporation throughout the retina (Koenig et al., 2016). This long pulse provided time for cells to move after incorporation, making it difficult to identify if only a subset of cells may be proliferative. To more precisely understand cell cycle state and organization in the early retina, we performed a 10 minute Brdu pulse experiment, fixing immediately, and co-labeling with phosphohistone H3 immunofluorescence (PH3) (Figure 1B). We see that BrdU incorporation in S-phase cells is restricted to the posterior of the retina after 10 minutes. We also find PH3 positive labeled nuclei, in late G2 and M phase, on the anterior surface of the retina, supporting previous observations. The lack of Brdu incorporation in the anterior retina suggests that some cells are already post-mitotic.

If cells are undergoing interkinetic nuclear migration, we would expect Brdu positive nuclei to eventually migrate apically to divide. To test this hypothesis, we chased our 10 minute BrdU pulse, sampling embryos every ten minutes for 110 minutes, again co-labeling with PH3 (Figure 1C). We found that at 80 minutes after the pulse we see BrdU positive/PH3 positive cells in the anterior retina, suggesting that nuclei are migrating apically to divide (Figure 1D). If proliferative cells in the posterior retina eventually exit the cell cycle and join the cells in the anterior retina, we would expect to find Brdu positive/PH3 negative cells in the anterior retina. Indeed, at 110 minutes we find BrdU positive, PH3 negative cells in the anterior retina (Figure 1E). Together, these data

102 suggest that cells in the cell cycle have nuclei residing in the posterior retina and these nuclei
103 migrate apically to divide. Eventually these cells exit the cell cycle and their cell bodies migrate to
104 the anterior of the retina. These data are consistent with cells undergoing interkinetic nuclear
105 migration, with post-mitotic cells segregated apically.
106
107 ***In vivo* observations of nuclear migration and proliferation in the squid retinal epithelium**
108 To better understand the dynamics of these cell behaviors, it is necessary to observe
109 development *in vivo*. This required us to develop a cell-resolution live-imaging protocol in
110 cephalopods (Figure 2A). We injected fluorescent Dextran to broadly label cell membranes and
111 performed >9 hour developmental time course experiments of the squid retina at stage 23 (Figure
112 2A). Within these time course datasets, we were able to track individual cells migrating from the
113 basal lamina to the apical side of the retina, mitose, and migrate basally again (Figure 2B, 2C,
114 Movie S1, S2, S3). These data confirm the process of interkinetic nuclear migration in the squid
115 retina. From these data we are able to calculate nuclear velocity, and were able to assess that
116 this migratory behavior is similar in velocity to movement described in the vertebrate retina
117 (Norden et al., 2009).
118 The molecular motors contributing to nuclear migration have been interrogated in a
119 number of developmental contexts and found that some tissues rely exclusively or primarily on
120 actomyosin, while others require microtubule contribution to promote migration (Kosodo, 2012; E.
121 J. Meyer et al., 2011; Norden, 2017). To understand the contribution of these motors to nuclear
122 migration in the squid retina, we have treated the embryos with actin polymerization inhibitor
123 cytochalasin D and microtubule polymerization inhibitor nocodazole for seven hours and fixed
124 immediately. The impact of these inhibitors on nuclear migration was assessed using
125 immunofluorescence for PH3 (Figure 2E-2H). We find that nuclei positive for PH3 in the
126 cytochalasin D treated retinas are often displaced from the mitotic zone (MZ), defined as the
127 region of the epithelia containing nuclei abutting the most apical membrane. We find a small
128 percentage of PH3 positive nuclei in controls are also outside the mitotic zone, which are likely at
129 the end of G2, migrating toward the apical surface. Quantifying these differences we see a
130 significant increase in cells outside the mitotic zone in our CytoD treated embryos suggesting
131 actin polymerization is required for nuclear migration. In addition, we also see defects in migration
132 in our nocodazole treated embryos. We see a population of PH3 positive nuclei that have
133 accumulated at the apical surface of the retina. This is what we would expect if microtubules were
134 not required for migration, as cells that have successfully migrated apically would then arrest and
135 accumulate in M phase as microtubules are required for mitosis. However, in addition to this

136 accumulation, we find a subpopulation of PH3 positive cells that are away from the mitotic zone,
137 suggesting that microtubules play some role in nuclear migration in the cephalopod retina.
138 In addition to nuclear movement, we were also able to assess the angle of cell division in
139 the epithelium. Symmetrical and asymmetrical cell division is an essential aspect of regulating
140 self-renewal, cell cycle exit and cell fate commitment during neurogenesis in multiple organisms
141 (Yu et al., 2006; Zigman et al., 2005; Dehay & Kennedy, 2007). Overwhelmingly, we find most
142 mitoses observed to be symmetrical relative to the apical surface of the epithelium (Figure 2I,
143 Movie S2). We hypothesize that these divisions are self-renewing. We also observe
144 approximately 10% of cell divisions to be angled relative to the apical surface (Figure 2I, 2J &
145 2K, Movie S3). We determined that symmetrical cell divisions had a division plane with an angle
146 relative to the apical surface between 60-90 degrees and asymmetrical divisions between 30-60
147 degrees (Figure 2K). We did not observe any cell divisions perpendicular to the apical surface,
148 (0-30 degrees) as have been observed in other systems (Knoblich, 2008; Morin & Bellaïche,
149 2011). We hypothesize that these asymmetric cell divisions may contribute to cells exiting the cell
150 cycle, however we were unable to follow cells long enough during live imaging to confirm this
151 hypothesis.
152
153 **Molecular identity during retinal neurogenesis**
154 To better understand the molecular state correlated with the cell cycle organization
155 observed in our BrdU and live imaging experiments, we sought to find molecular markers that
156 help define differentiation trajectories in the cephalopod retina. We analyzed spatiotemporal
157 expression of candidate neurogenesis markers in the retina (Figure 3A, Supplemental Figure 1).
158 We identified that in early retinal development, stage 21, *DpSoxB1* is homogeneously expressed
159 across the retinal epithelium. At stage 23 the retina is divided across the apical-basal axis with
160 *DpSoxB1* found on the basal side of the retina, correlating with Brdu incorporation, and *DpEphR*
161 expressed on the apical side. At stage 25 we see the maintenance of segregated *DpSoxB1* and
162 *DpEphR* expression, as well as the first evidence of the terminal differentiation markers
163 *DpRetinochrome* and *DpRhodopsin*. At stage 27, the first evidence of the basal membrane is
164 apparent. At this stage we see a loss of strict segregation of *DpSoxB1* and *DpEphR* expression.
165 We hypothesize this change is a result of cell-body migration or mixing, with apical cells moving
166 to the posterior of the retina and basal cells moving to the anterior of the retina. We hypothesize
167 that this resorting moves the post-mitotic cells to the posterior where they will become the first
168 photoreceptor cell bodies to migrate behind the basal membrane. Supporting this hypothesis, we
169 find that *DpSoxB1* expression is never found posterior to the basal membrane. However, *DpEphR*

170 is found on both sides of the membrane until hatching. At hatching *DpEphR* is isolated to a subset
171 of cells posterior to the basal membrane. These cells may be maturing photoreceptor cells that
172 have recently migrated to the photoreceptor cell layer during hatching and post-hatching stage
173 growth. Terminal differentiation markers span both sides of the basal membrane at hatching. We
174 hypothesize that *DpRhodopsin* is expressed exclusively in the photoreceptor cells and is being
175 trafficked to the outer segment and that *DpRetinochrome* is expressed in both the photoreceptor
176 cells and support cells.
177 This candidate gene survey suggests cell differentiation trajectories in the retina (Figure
178 3B, 3C). Our photoreceptor cell differentiation trajectory starts as *DpSoxB1* positive retinal
179 progenitor cells undergoing interkinetic nuclear migration in the pseudostratified epithelium.
180 These cells transition to *DpEphR* positive cells and become post-mitotic. Eventually *DpEphR*
181 expressing cells mature and begin to express terminal differentiation markers, ultimately
182 completing differentiation when they exclusively express *DpRhodopsin* and *DpRetinochrome.*
183 We hypothesize a simple differentiation trajectory for the proliferative support cell
184 population (Figure 3B & 3C). These cells start as *DpSoxB1* positive retinal progenitor cells,
185 undergoing interkinetic nuclear migration. This self-renewing population is maintained throughout
186 development. During cell mixing at stage 27, *DpSoxB1* positive support cells begin to express
187 *DpRetinochrome,* migrate anterior in the retina and remain in the cell cycle. The
188 *DpSoxB1/DpRetinochrome* expressing support cells may be a long term stem cell population in
189 the retina.
190
191 **Notch regulates retinal progenitor identity in the cephalopod**
192 Our data shows that BrdU incorporation correlates with *DpSoxB1* expression and *DpEphR*
193 expression correlates with post mitotic cells. Our Brdu chase experiments suggest that *DpSoxB1*
194 cells likely become *DpEphR* cells over time (Figure 4A, 4B & 4C). Notch signaling is a well known
195 regulator of cell cycle exit and differentiation. Previous work showed that inhibiting Notch signaling
196 in the cephalopod using the gamma-secretase inhibitor DAPT, led to a loss of BrdU incorporation
197 in the retina, showing that Notch was regulating cell cycle exit. We were interested in
198 understanding the role of Notch signaling in regulating cell fate trajectories in conjunction with
199 proliferation. We first performed *in situ* hybridization for Notch signaling pathway members in the
200 retina (Figure 4D and Supplemental Figure 2). If Notch signaling is important for maintaining
201 progenitor fate, we would expect Notch and Hes to be enriched in retinal progenitor cells. We find
202 that *DpNotch* and *DpHes-1* expression is correlated with *DpSoxB1* expression and retinal
203 progenitor identity (Figure 4D and Supplemental Figure 2). Interestingly, we find that Delta is

204 ubiquitously expressed during these stages (Supplemental Figure 2). We also find *DpNotch*
205 expressed in a limited number of nuclei on the apical side of the retina. We wanted to know if this
206 expression correlated with nuclei that had migrated apically to divide. We performed *in situ*
207 hybridization for *DpNotch* in conjunction with PH3 immunofluorescence and found that apical
208 *DpNotch* expression is correlated with PH3 positive nuclei (Figure 4E). Inheritance of Notch
209 mRNA may be an important part of maintaining progenitor cell identity.

210 To assess the role of Notch in cell fate we again used the gamma secretase inhibitor
211 DAPT to inhibit active signaling. Embryos were treated with DAPT or DMSO starting at stage 23
212 for 24 hours. Eyes were dissected and pooled. RNA was extracted from three experimental and
213 control samples and sequenced. 2242 genes were differentially expressed between DAPT and
214 control eyes with a p-value of less than 0.05 (Supplemental Table 1). *DpSoxB1* was found
215 downregulated and *DpEphR* was found upregulated in the dataset but these changes were not
216 deemed statistically significant. DAPT compared to control eye samples showed changes, both
217 up and down regulation, in neural and sensory markers. Of note is the down regulation of
218 Rhodopsin and other G-protein coupled receptor related genes (Figure 4F). In addition cell cycle
219 related genes showed downregulation, which is expected as DAPT treatment leads to cell cycle
220 exit in the squid retina (Koenig et al., 2016) (Figure 4G). Finally, DAPT versus control eyes
221 showed significant changes in cell signaling genes, suggesting that Notch may self-regulate as
222 well as interact with other signaling pathways in the retina, including VEGFR, BMP and Wnt
223 (Figure 4H).

224 To confirm changes in gene expression identified in the RNA-seq analysis, we performed
225 *in situ* hybridization studies on control and DAPT embryos (Figure 4I and Supplemental Figure 3
226 and Supplemental Figure 4). We confirm trends shown in the RNA-seq results. Specifically, we
227 find a loss of *DpNotch* expression, a downregulation of *DpRhodopsin,* and a complete loss of
228 *DpSoxB1* in DAPT treated retinas (Figure 4I). We also observe a gain of expression of *DpEphR*
229 and synaptic transmission related gene, *DpSec-1,* in the posterior retina (Figure 4I). Interestingly,
230 we see ectopic expression of VEGFR in a subpopulation of cells in the DAPT treated retinas
231 relative to control. The inconsistent and unclear placement may be compounded by the
232 disorganization of the DAPT treated retinas. The complete loss of *DpSoxB1* and the ectopic
233 expression of *DpEphR* shows that DAPT inhibition not only results in changes in cell cycle state,
234 but also changes molecular fate in the squid retina. These data suggest that Notch signaling is
235 required to maintain retinal progenitor identity in the squid.
236

237 **Discussion**

238 In the current study we have characterized the oscillatory behaviors of retinal progenitor
239 cells in squid. We have defined the molecular markers for progenitor, post-mitotic, and fully
240 differentiated cells in the retina and and we have shown that Notch signaling is regulating both
241 cell cycle and molecular identity during retinal development. The importance of these findings is
242 in comparison to what is known about neurogenesis in other systems.

243 Pseudostratified epithelia and interkinetic nuclear migration have been observed in
244 multiple tissue types and across multiple species (E. J. Meyer et al., 2011). In the nervous system,
245 pseudostratification was historically considered a vertebrate specific developmental trait, and
246 responsible for the large size of the central nervous system. Elaborate tissue-level morphogenesis
247 is not usually observed in invertebrate neural development, where individual cells delaminate or
248 ingress from a simple or stratified neuroepithelium, sometimes divide, and then migrate to their
249 final destination to differentiate (N. P. Meyer & Seaver, 2009; Sur et al., 2020; Byrne, 2019;
250 Hartenstein & Stollewerk, 2015). However interkinetic nuclear migration has now been described
251 in the *Drosophila* optic lobe (Egger et al., 2007). In this case, the apicobasal distance of migration
252 is significantly smaller than other vertebrate neurogenic tissues and cells delaminate from the
253 edge of the proliferative epithelium and migrate to their final destination to differentiate (Egger et
254 al., 2007; Holguera & Desplan, 2018; Strzyz et al., 2016). This process has been compared to
255 "conveyor belt" neurogenesis found in the zebrafish ciliary and tectal marginal zones, where,
256 during long term growth, cells are progressively added from the edge of a pseudostratified stem
257 cell population (Joly et al., 2016). The behavior described in the squid retina is unusual because
258 of its unique similarity to early neurogenesis in vertebrate species, which is characterized by
259 waves of differentiation within the pseudostratified epithelium (Agathocleous & Harris, 2009;
260 Livesey & Cepko, 2001). In the squid, apicobasal height of the epithelium is similar to vertebrate
261 tissues, cells undergo interkinetic nuclear migration while proliferative, and remain within the
262 bounds of the epithelium after delaminating and differentiating. The functional difference between
263 conveyor belt neurogenesis versus within epithelium differentiation is unclear but the architecture
264 of the epithelium may provide physical landmarks or signaling information important for proper
265 organization.

266 Although pseudostratified neurogenesis is found in the cephalopod retina, there is little
267 evidence that the cell biology of chordal or central nervous system neurogenesis is similar. It has
268 been reported that cells migrate from the lateral lip in the cephalopod embryo to regions within
269 the brain (Deryckere et al., 2021). However, no pseudostratification of the lateral lips has been
270 described. Cephalopod central nervous system development may more closely resemble
271 neurogenesis found in other invertebrates or molluscs (Deryckere et al., 2021; Marthy, 1987).

272 However, with a central nervous system composed of significantly more cells than other Spiralians
273 and requiring long distance cell migration, it is likely that cephalopods have evolved lineage
274 specific mechanisms to manage this process.

275 Interestingly, in the squid, candidate gene expression of neurogenic factors also differs
276 significantly between the developing retina and other brain regions. This includes a lack of
277 expression of the canonical neurogenic ELAV, *DpElav-1,* in the retina, an RNA binding protein
278 commonly found in differentiating neurons across species (Akamatsu et al., 2005; Denes et al.,
279 2007; N. P. Meyer & Seaver, 2009; Nakanishi et al., 2012; Nomaksteinsky et al., 2009). bHLH
280 factors NeuroD and NeuroG, which both have roles in neural specification and differentiation in
281 many animals and are expressed in the lateral lips and brain in *D. pealeii* and other cephalopods,
282 are completely absent for the retina (Supplemental Figure 1) (Buresi et al., 2013; Deryckere et
283 al., 2021; Shigeno et al., 2015). However, it has been reported in *Octopus vulgaris* that achaete-
284 scute homolog *Ov-ascl1*, a third proneural bHLH transcription factor, is expressed in the retina
285 (Deryckere et al., 2021). Furthermore, SoxB1, required to maintain neural precursors cells in
286 vertebrates (Sox1, 2 and 3) and neuroblasts in *Drosophila* (SoxNeuro and Dichaete), is also a
287 retinal progenitor marker in cephalopods (Buescher et al., 2002; Bylund et al., 2003; Ferrero et
288 al., 2014; Holmberg et al., 2008; Overton et al., 2002; Taranova et al., 2006). We also find that
289 both cephalopod-specific ELAV paralogs, *DpElav-2* and *DpElav-3*, show expression that
290 suggests a role in neurogenesis in both the retina and brain (Supplemental Figure 1).

291 Finally, we show that Notch signaling is maintaining molecular identity of the progenitor
292 population in the squid retina, and that the loss of Notch signaling leads to expression of the post-
293 mitotic marker *DpEphR*. In the vertebrate retina, the premature loss of Notch signaling leads to
294 the differentiation of early born cell types (Perron & Harris, 2000). In *D. pealeii*, we see a decrease
295 in *DpRhodopsin* expression, suggesting cells may have arrested in this immature post-mitotic
296 state. We also see the maintenance in *DpRetinochrome* expression, which may be evidence of
297 differing trajectories of these cell types during neurogenesis.

298 The function of pseudostratification and interkinetic nuclear migration during development
299 still remains unclear, however our data sheds new light on old hypotheses. In particular,
300 pseudostratification may aid in intracellular organization, as we see significant mRNA localization
301 in our data, including mRNA transport correlated with nuclear migration. It may also be that the
302 physics and dynamics of pseudostratified epithelia is better at accommodating increased
303 proliferation or provides an organizational scaffold for the differentiating network of neurons. It will
304 be interesting to apply new fluid dynamics approaches used to study vertebrate neurogenesis to
305 the cell biology of this similar tissue (Azizi et al., 2020) . Ultimately, the evidence we have

306 generated in cephalopods suggest that vertebrate-like cell behaviors during neurogenesis is not
307 exclusive to the deuterostome lineage, and with greater sampling we may better understand the
308 evolutionary changes that contribute to the diversity and complexity we see.
309
310
311 **Methods**
312 **Animal Husbandry**
313 *Doryteuthis pealeii* egg sacks were obtained from the Marine Biological Labs. Egg sacks were
314 kept at 20 degrees Celsius in 20 gallon aquaria in artificial seawater under a day night cycle.
315 Although not required, European guidelines for cephalopod research were followed.
316
317 **Cloning and *in situ* Hybridization**
318 Primers were designed using Primer3 in the Geneious software package version 2020.04
319 (https://www.geneious.com) and primer sequences are reported in Supplemental Table 2. Genes
320 were cloned into pGEM-T Easy vector and confirmed with sanger sequencing and DIG-labeled
321 RNA probes were synthesized as previously reported (Koenig et al., 2016). Embryos were fixed
322 overnight at 4 degrees celsius, washed and dehydrated stepwise into 100% ethanol. Embryos
323 were embedded, paraffin sectioned and *in situ* hybridization was performed as previously reported
324 (Neal et al., n.d.). All *in situs* were replicated in at least three embryos across multiple separate *in*
325 *situ* experiments. Slides were stained overnight with Sytox-Green 1:1000 overnight, mounted
326 using ImmunoHistoMount (Abcam) and imaged on a Zeiss Axioskop 2.
327
328 **Brdu Experiments**
329 Embryos were bathed in BrdU (10 mM) in pen-strep seawater for 10 minutes as previously
330 described (Koenig et al., 2016). Embryos were fixed immediately and the remaining embryos
331 were moved into pen-strep seawater. Groups of 10-15 embryos were fixed every ten minutes for
332 two hours. Embryos were fixed overnight at 4 degrees and washed out into PBS-Tween. Embryos
333 were stepped into 30% sucrose and embedded in tissue freezing medium and sectioned as
334 previously described (Koenig et al., 2016)). Antigen-retrieval and immunofluorescence was
335 performed as previously described. Brdu antibody (Abcam ab6326) at concentration 1:250.
336 Phosphohistone H3 antibody (Sigma-Aldrich 06-570) was used at concentration 1:300.
337 Secondary antibodies goat anti-rat Alexa Fluor 488 and goat anti rabbit Alexa Fluor 647
338 (Invitrogen). Sections were counterstained with Sytox Green at 1:1000. Sections were imaged on
339 a Zeiss LSM 880 or Zeiss LSM 980.

340

341 **Live-imaging experiments**

342 Embryos were dissected from egg cases. The vitreous space was injected using a pico-liter
343 microinjector with Dextran Alexa Fluor 488 10,000 MW (D22910) at stage 23. Embryos were
344 embedded in 1% low melt agarose in seawater and mounted in cover glass bottom dishes
345 (100503-366). Embryos were immersed in pen strep seawater. Embryos were imaged on a Zeiss
346 880. Embryos were imaged every ten minutes for at least nine hours.

347

348 **Imaging analysis**

349 Image analysis was performed in Fiji (Schindelin et al., 2012). Intensity range was adjusted in Fiji
350 to better identify cell membranes. Drift correction was performed using Fiji plugin CoordinateShift
351 (written by Housei Wada, https://signaling.riken.jp/en/en-tools/imagej/). Nuclear tracking was
352 performed both manually and using Fiji plugin Trackmate (Robertson, 2018; Schindelin et al.,
353 2012). Tracks were visualized and distance and velocity measurements were obtained from
354 Trackmate and plotted graphically, normalizing to the highest point in migration.

355

356 ***Ex ovo* and Drug Treatments**

357 Embryos were treated in 20uM DAPT solution or DMSO control in filter-sterilized, Pen-Strep
358 seawater starting at stage 23 for 24 hours and fixed immediately as previously described (Koenig
359 et. al, 2016). Embryos were bathed in 5uM Nocodazole (M1404-2MG, Sigma-Aldrich) and 5uM
360 Cytochalasin D (C8273-1MG, Sigma-Aldrich)for 7 hours and fixed immediately.

361

362 **RNA-seq and Bioinformatics**

363 Stage 23 embryos were treated with the gamma-secretase inhibitor DAPT at 20um in filter
364 sterilized sea water for 24 hours and Control embryos were treated with the equivalent amount of
365 DMSO, as previously described (Koenig et al., 2016). DAPT and Control eyes were dissected,
366 pooled and macerated in Trizol and stored at -80 degrees Celsius. RNA was extracted using a
367 standard TRIzol (Invitrogen #15596026) chloroform extraction and passed through a gDNA
368 eliminator mini-spin column (Qiagen #1030958). RNA was precipitated with isopropanol and then
369 again precipitated with ethanol and checked for quality. Library prep and sequencing was
370 performed at the Bauer Core at Harvard University. RNA-seq libraries were generated using the
371 Kapa mRNA-Hyper Prep kit with Poly-A Selection (Roche, Basal) and were sequenced on the
372 Illumina NovaSeq (>70 million 2x150 bp sequences) (Illumina, San Diego, CA).

373 Sequence quality control was performed according to the best practice recommendation
374 on the Harvard FAS Informatics pipeline (https://informatics.fas.harvard.edu/best-practices -for-
375 de-novo-transcriptome-assembly-with-trinity.html). Erroneous kmers were removed from the
376 paired end Illumina dataset using rCorrector. Reads with Ns or other low complexity pairs were
377 removed using a custom python script provided by the Harvard Informatics GitHub
378 (FilterUncorrectabledPEfastq.py). Adapters and low quality bases were removed using
379 TrimGalore! Reads that mapped using Bowtie2 to the rRNA databases SILVA 132 SSURef Nr99
380 tax and SILVA 132 LSUParc tax were removed. Pseudomapping was performed by Kallisto with
381 100 bootstraps to a previously published whole embryo transcriptome (Koenig et al., 2016).
382 Transcript abundances were imported using tximport (https://bioconductor.org/packages/3.7/ b
383 ioc/vignettes/tximport/inst/doc/tximport.html#use-with-downstream-bioconductor-dge-packages)
384 into DESeq2 using the Kallisto abundance.h5 files. Differential gene expression was determined
385 by importing transcript level abundances and gene level offset using
386 *DESeqDataSetFromTximport* (Soneson et al., 2015). The DESeq2 pipeline was run and
387 differentially expressed genes were considered with a p value of .05 and log2 fold change of
388 above 1 and below -1. All genes shown in the chord plots in figure 4 meet these criteria with the
389 exception of Notch which was included with a log2 fold change of -0.83. GO annotations were
390 identified using the DAVID functional annotation tool (Huang et al., 2007). Chord plots were
391 generated using the R package GOPlot (Walter et al., 2015) and gplots (*Website*,
392 n.d.)Warnes(*Website*, n.d.).
393
394
395 **Funding**
396 This work was supported by a grant from the Office of the NIH Director 1DP5OD023111-01 and
397 the John Harvard Distinguished Science Fellowship awarded to K.M.K.
398
399 **Acknowledgements**
400 We would like to thank the Srivastava lab for helpful discussions and Mansi Srivastava and Jeffrey
401 Gross for comments on the manuscript. We thank Kevin Woods and the John Harvard
402 Distinguished Science Fellows community for support and the Marine Biological Labs and the
403 Marine Resources Center for assistance and access to embryos.
404
405 **Author Contributions**

K.M.K conceived of the study with input from F.N., C.M.D. and S.N.; K.M.K, F.N., C.M.D., S.N., A.Z., and A.L. performed experiments. K.J.M. performed phylogenetic analyses. K.M.K., C.M.D and K.J.M. wrote the manuscript in consultation with all authors.

References

Agathocleous, M., & Harris, W. A. (2009). From Progenitors to Differentiated Cells in the Vertebrate Retina. In *Annual Review of Cell and Developmental Biology* (Vol. 25, Issue 1, pp. 45–69). https://doi.org/10.1146/annurev.cellbio.042308.113259

Akamatsu, W., Fujihara, H., Mitsuhashi, T., Yano, M., Shibata, S., Hayakawa, Y., Okano, H. J., Sakakibara, S.-I., Takano, H., Takano, T., Takahashi, T., Noda, T., & Okano, H. (2005). The RNA-binding protein HuD regulates neuronal cell identity and maturation. *Proceedings of the National Academy of Sciences of the United States of America*, *102*(12), 4625–4630. https://doi.org/10.1073/pnas.0407523102

Arnold, J. M. (1965). NORMAL EMBRYONIC STAGES OF THE SQUID, LOLIGO PEALII (LESUEUR). In *The Biological Bulletin* (Vol. 128, Issue 1, pp. 24–32). https://doi.org/10.2307/1539386

Azizi, A., Herrmann, A., Wan, Y., Buse, S. J., Keller, P. J., Goldstein, R. E., & Harris, W. A. (2020). Nuclear crowding and nonlinear diffusion during interkinetic nuclear migration in the zebrafish retina. *eLife*, *9*. https://doi.org/10.7554/eLife.58635

Baye, L. M., & Link, B. A. (2008). Nuclear migration during retinal development. In *Brain Research* (Vol. 1192, pp. 29–36). https://doi.org/10.1016/j.brainres.2007.05.021

Bertrand, V., & Hobert, O. (2010). Lineage programming: navigating through transient regulatory states via binary decisions. *Current Opinion in Genetics & Development*, *20*(4), 362–368. https://doi.org/10.1016/j.gde.2010.04.010

Buescher, M., Hing, F. S., & Chia, W. (2002). Formation of neuroblasts in the embryonic central nervous system of Drosophila melanogaster is controlled by SoxNeuro. *Development* ,

433 *129*(18), 4193–4203. https://www.ncbi.nlm.nih.gov/pubmed/12183372
434 Buresi, A., Canali, E., Bonnaud, L., & Baratte, S. (2013). Delayed and asynchronous ganglionic
435 maturation during cephalopod neurogenesis as evidenced by Sof-elav1 expression in
436 embryos of Sepia officinalis (Mollusca, Cephalopoda). *The Journal of Comparative*
437 *Neurology*, *521*(7), 1482–1496. https://doi.org/10.1002/cne.23231
438 Bylund, M., Andersson, E., Novitch, B. G., & Muhr, J. (2003). Vertebrate neurogenesis is
439 counteracted by Sox1–3 activity. In *Nature Neuroscience* (Vol. 6, Issue 11, pp. 1162–1168).
440 https://doi.org/10.1038/nn1131
441 Byrne, J. H. (2019). *The Oxford Handbook of Invertebrate Neurobiology*. Oxford University
442 Press. https://play.google.com/store/books/details?id=O_iEDwAAQBAJ
443 Dehay, C., & Kennedy, H. (2007). Cell-cycle control and cortical development. In *Nature*
444 *Reviews Neuroscience* (Vol. 8, Issue 6, pp. 438–450). https://doi.org/10.1038/nrn2097
445 Denes, A. S., Jékely, G., Steinmetz, P. R. H., Raible, F., Snyman, H., Prud'homme, B., Ferrier,
446 D. E. K., Balavoine, G., & Arendt, D. (2007). Molecular architecture of annelid nerve cord
447 supports common origin of nervous system centralization in bilateria. *Cell*, *129*(2), 277–288.
448 https://doi.org/10.1016/j.cell.2007.02.040
449 Deryckere, A., Styfhals, R., Elagoz, A. M., Maes, G. E., & Seuntjens, E. (2021). Identification of
450 neural progenitor cells and their progeny reveals long distance migration in the developing
451 octopus brain. *eLife*, *10*. https://doi.org/10.7554/eLife.69161
452 Egger, B., Boone, J. Q., Stevens, N. R., Brand, A. H., & Doe, C. Q. (2007). Regulation of
453 spindle orientation and neural stem cell fate in the Drosophila optic lobe. *Neural*
454 *Development*, *2*, 1. https://doi.org/10.1186/1749-8104-2-1
455 Ferrero, E., Fischer, B., & Russell, S. (2014). SoxNeuro orchestrates central nervous system
456 specification and differentiation in Drosophila and is only partially redundant with Dichaete.
457 *Genome Biology*, *15*(5), R74. https://doi.org/10.1186/gb-2014-15-5-r74
458 Gagnon, Y. L., Sutton, T. T., & Johnsen, S. (2013). Visual acuity in pelagic fishes and mollusks.

Vision Research, *92*, 1–9. https://doi.org/10.1016/j.visres.2013.08.007

Hartenstein, V., & Stollewerk, A. (2015). The evolution of early neurogenesis. *Developmental Cell*, *32*(4), 390–407. https://doi.org/10.1016/j.devcel.2015.02.004

Holguera, I., & Desplan, C. (2018). Neuronal specification in space and time. *Science*, *362*(6411), 176–180. https://doi.org/10.1126/science.aas9435

Holmberg, J., Hansson, E., Malewicz, M., Sandberg, M., Perlmann, T., Lendahl, U., & Muhr, J. (2008). SoxB1 transcription factors and Notch signaling use distinct mechanisms to regulate proneural gene function and neural progenitor differentiation. *Development* , *135*(10), 1843–1851. https://doi.org/10.1242/dev.020180

Huang, D. W., Sherman, B. T., Tan, Q., Kir, J., Liu, D., Bryant, D., Guo, Y., Stephens, R., Baseler, M. W., Clifford Lane, H., & Lempicki, R. A. (2007). DAVID Bioinformatics Resources: expanded annotation database and novel algorithms to better extract biology from large gene lists. In *Nucleic Acids Research* (Vol. 35, Issue suppl_2, pp. W169–W175). https://doi.org/10.1093/nar/gkm415

Joly, J.-S., Recher, G., Brombin, A., Ngo, K., & Hartenstein, V. (2016). A Conserved Developmental Mechanism Builds Complex Visual Systems in Insects and Vertebrates. *Current Biology: CB*, *26*(20), R1001–R1009. https://doi.org/10.1016/j.cub.2016.08.017

Knoblich, J. A. (2008). Mechanisms of asymmetric stem cell division. *Cell*, *132*(4), 583–597. https://doi.org/10.1016/j.cell.2008.02.007

Koenig, K. M., & Gross, J. M. (2020). Evolution and development of complex eyes: a celebration of diversity. *Development* , *147*(19). https://doi.org/10.1242/dev.182923

Koenig, K. M., Sun, P., Meyer, E., & Gross, J. M. (2016). Eye development and photoreceptor differentiation in the cephalopod Doryteuthis pealeii. *Development* , *143*(17), 3168–3181. https://doi.org/10.1242/dev.134254

Kosodo, Y. (2012). Interkinetic nuclear migration: beyond a hallmark of neurogenesis. *Cellular and Molecular Life Sciences: CMLS*, *69*(16), 2727–2738. https://doi.org/10.1007/s00018-

012-0952-2

Livesey, F. J., & Cepko, C. L. (2001). Vertebrate neural cell-fate determination: lessons from the retina. *Nature Reviews. Neuroscience*, *2*(2), 109–118. https://doi.org/10.1038/35053522

Marthy, H.-J. (1987). Ontogenesis of the Nervous System in Cephalopods. In *Nervous Systems in Invertebrates* (pp. 443–459). https://doi.org/10.1007/978-1-4613-1955-9_15

Meyer, E. J., Ikmi, A., & Gibson, M. C. (2011). Interkinetic Nuclear Migration Is a Broadly Conserved Feature of Cell Division in Pseudostratified Epithelia. In *Current Biology* (Vol. 21, Issue 6, pp. 485–491). https://doi.org/10.1016/j.cub.2011.02.002

Meyer, N. P., & Seaver, E. C. (2009). Neurogenesis in an annelid: Characterization of brain neural precursors in the polychaete Capitella sp. I. In *Developmental Biology* (Vol. 335, Issue 1, pp. 237–252). https://doi.org/10.1016/j.ydbio.2009.06.017

Morin, X., & Bellaïche, Y. (2011). Mitotic spindle orientation in asymmetric and symmetric cell divisions during animal development. *Developmental Cell*, *21*(1), 102–119. https://doi.org/10.1016/j.devcel.2011.06.012

Nakanishi, N., Renfer, E., Technau, U., & Rentzsch, F. (2012). Nervous systems of the sea anemone Nematostella vectensis are generated by ectoderm and endoderm and shaped by distinct mechanisms. *Development* , *139*(2), 347–357. https://doi.org/10.1242/dev.071902

Neal, S., McCulloch, K. J., Napoli, F., Daly, C. M., Coleman, J. H., & Koenig, K. M. (n.d.). *Co-option of the Limb Patterning Program in Cephalopod Lens Development*. https://doi.org/10.1101/2021.04.22.441006

Nomaksteinsky, M., Röttinger, E., Dufour, H. D., Chettouh, Z., Lowe, C. J., Martindale, M. Q., & Brunet, J.-F. (2009). Centralization of the deuterostome nervous system predates chordates. *Current Biology: CB*, *19*(15), 1264–1269. https://doi.org/10.1016/j.cub.2009.05.063

Norden, C. (2017). Pseudostratified epithelia – cell biology, diversity and roles in organ

formation at a glance. In *Journal of Cell Science*. https://doi.org/10.1242/jcs.192997

Norden, C., Young, S., Link, B. A., & Harris, W. A. (2009). Actomyosin is the main driver of interkinetic nuclear migration in the retina. *Cell*, *138*(6), 1195–1208. https://doi.org/10.1016/j.cell.2009.06.032

Overton, P. M., Meadows, L. A., Urban, J., & Russell, S. (2002). Evidence for differential and redundant function of the Sox genes Dichaete and SoxN during CNS development in Drosophila. *Development* , *129*(18), 4219–4228. https://www.ncbi.nlm.nih.gov/pubmed/12183374

Packard, A. (1972). CEPHALOPODS AND FISH: THE LIMITS OF CONVERGENCE. In *Biological Reviews* (Vol. 47, Issue 2, pp. 241–307). https://doi.org/10.1111/j.1469-185x.1972.tb00975.x

Perron, M., & Harris, W. A. (2000). Determination of vertebrate retinal progenitor cell fate by the Notch pathway and basic helix-loop-helix transcription factors. *Cellular and Molecular Life Sciences: CMLS*, *57*(2), 215–223. https://doi.org/10.1007/PL00000685

Robertson, R. (2018). *Open and Extensible Control & Analytics Platform for Synchrophasor Data*. https://doi.org/10.2172/1468940

Schindelin, J., Arganda-Carreras, I., Frise, E., Kaynig, V., Longair, M., Pietzsch, T., Preibisch, S., Rueden, C., Saalfeld, S., Schmid, B., Tinevez, J.-Y., White, D. J., Hartenstein, V., Eliceiri, K., Tomancak, P., & Cardona, A. (2012). Fiji: an open-source platform for biological-image analysis. *Nature Methods*, *9*(7), 676–682. https://doi.org/10.1038/nmeth.2019

Shigeno, S., Parnaik, R., Albertin, C. B., & Ragsdale, C. W. (2015). Evidence for a cordal, not ganglionic, pattern of cephalopod brain neurogenesis. In *Zoological Letters* (Vol. 1, Issue 1). https://doi.org/10.1186/s40851-015-0026-z

Soneson, C., Love, M. I., & Robinson, M. D. (2015). Differential analyses for RNA-seq: transcript-level estimates improve gene-level inferences. *F1000Research*, *4*, 1521.

https://doi.org/10.12688/f1000research.7563.2

Strzyz, P. J., Matejcic, M., & Norden, C. (2016). Heterogeneity, Cell Biology and Tissue Mechanics of Pseudostratified Epithelia: Coordination of Cell Divisions and Growth in Tightly Packed Tissues. *International Review of Cell and Molecular Biology*, *325*, 89–118. https://doi.org/10.1016/bs.ircmb.2016.02.004

Sur, A., Renfro, A., Bergmann, P. J., & Meyer, N. P. (2020). Investigating cellular and molecular mechanisms of neurogenesis in Capitella teleta sheds light on the ancestor of Annelida. *BMC Evolutionary Biology*, *20*(1), 84. https://doi.org/10.1186/s12862-020-01636-1

Taranova, O. V., Magness, S. T., Fagan, B. M., Wu, Y., Surzenko, N., Hutton, S. R., & Pevny, L. H. (2006). SOX2 is a dose-dependent regulator of retinal neural progenitor competence. *Genes & Development*, *20*(9), 1187–1202. https://doi.org/10.1101/gad.1407906

Taverna, E., Götz, M., & Huttner, W. B. (2014). The cell biology of neurogenesis: toward an understanding of the development and evolution of the neocortex. *Annual Review of Cell and Developmental Biology*, *30*, 465–502. https://doi.org/10.1146/annurev-cellbio-101011-155801

Walter, W., Sánchez-Cabo, F., & Ricote, M. (2015). GOplot: an R package for visually combining expression data with functional analysis: Fig. 1. In *Bioinformatics* (Vol. 31, Issue 17, pp. 2912–2914). https://doi.org/10.1093/bioinformatics/btv300

Website. (n.d.). Gregory R. Warnes, Ben Bolker, Lodewijk Bonebakker, Robert Gentleman, Wolfgang Huber, Andy Liaw, Thomas Lumley, Martin Maechler, Arni Magnusson, Steffen Moeller, Marc Schwartz and Bill Venables (2015). gplots: Various R Programming Tools for Plotting Data. R package version 2.17.0. http://CRAN.R-project.org/package=gplots

Yamamoto, T., Tasaki, K., Sugawara, Y., & Tonosaki, A. (1965). FINE STRUCTURE OF THE OCTOPUS RETINA. *The Journal of Cell Biology*, *25*, 345–359. https://www.ncbi.nlm.nih.gov/pubmed/14287185

Young, J. Z. (1974). The central nervous system of Loligo. I. The optic lobe. *Philosophical*

Transactions of the Royal Society of London. Series B, Biological Sciences, *267*(885), 263–302. https://doi.org/10.1098/rstb.1974.0002

Yu, F., Kuo, C. T., & Jan, Y. N. (2006). Drosophila Neuroblast Asymmetric Cell Division: Recent Advances and Implications for Stem Cell Biology. In *Neuron* (Vol. 51, Issue 1, pp. 13–20). https://doi.org/10.1016/j.neuron.2006.06.016

Zechner, C., Nerli, E., & Norden, C. (2020). Stochasticity and determinism in cell fate decisions. *Development* , *147*(14). https://doi.org/10.1242/dev.181495

Zigman, M., Cayouette, M., Charalambous, C., Schleiffer, A., Hoeller, O., Dunican, D., McCudden, C. R., Firnberg, N., Barres, B. A., Siderovski, D. P., & Knoblich, J. A. (2005). Mammalian inscuteable regulates spindle orientation and cell fate in the developing retina. *Neuron*, *48*(4), 539–545. https://doi.org/10.1016/j.neuron.2005.09.030

Gregory R. Warnes, Ben Bolker, Lodewijk Bonebakker, Robert Gentleman, Wolfgang Huber, Andy Liaw, Thomas Lumley, Martin Maechler, Arni Magnusson, Steffen Moeller, Marc Schwartz and Bill Venables (2015). gplots: Various R Programming Tools for Plotting Data. R package version 2.17.0. http://CRAN.R-project.org/package=gplots

580 **Figures and Figure Legends**

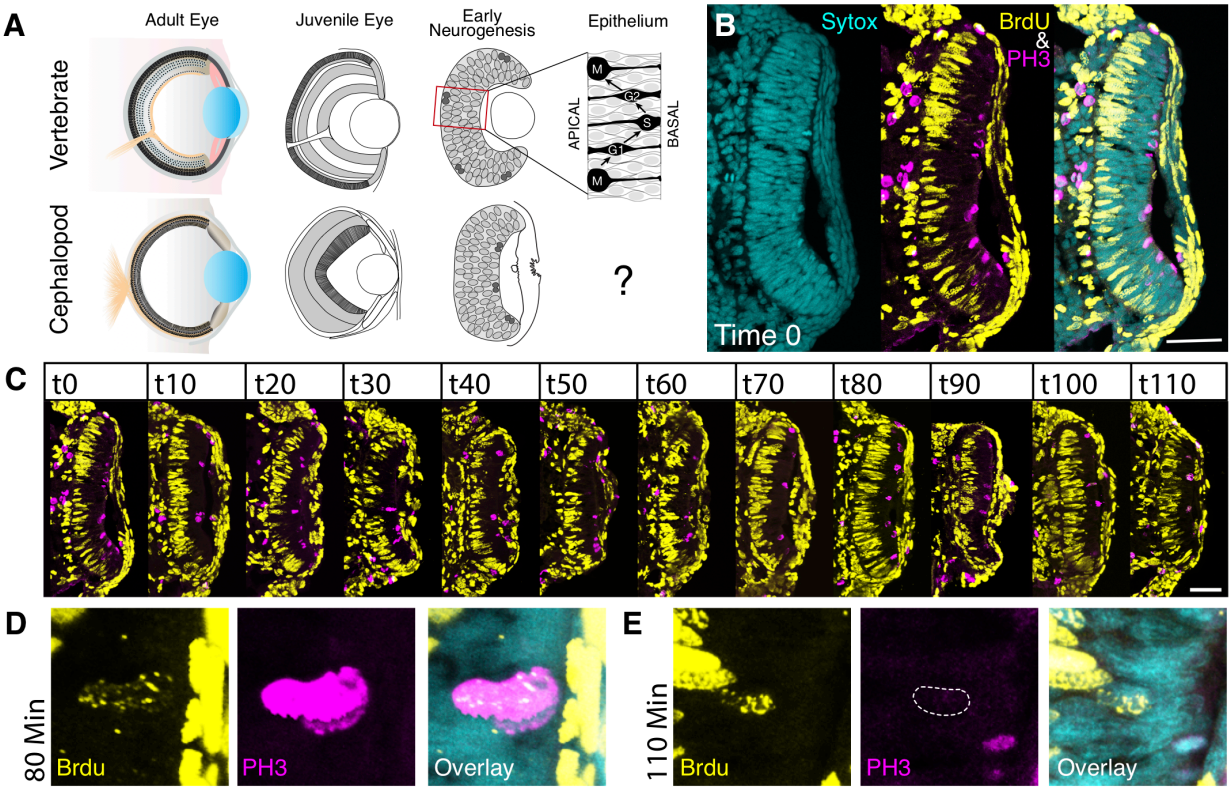

581 **Figure 1: Cell cycle and nuclear migration in the squid retina assessed in fixed tissue. A.**
582 Schematic of the vertebrate and cephalopod eye at adult, juvenile and early stage development. Box shows
583 enlargement of the vertebrate pseudostratified epithelium, apical to the left. Grey ovals are the nuclei
584 distributed across the tissue, darker nuclei are undergoing mitosis. **B.** 10 minute BrdU pulse and immediate
585 fix (Time 0) BrdU/PH3 antibody stain shows BrdU incorporation on the posterior side of the epithelium (S-
586 phase) and PH3 stain on the anterior side of the epithelium (M-phase). Scale 50um. **C.** BrdU/PH3 time
587 course. 10 minute BrdU pulse, fixed every 10 minutes followed by BrdU/PH3 antibody stains. Scale 50um.
588 Cell mixing is not observed until 80 minutes after pulse. **D.** 80 minutes after BrdU pulse is the first timepoint
589 where BrdU+/PH3+ nuclei are found on the apical side of the retina. **E.** 110 minutes after pulse is the first
590 time point where BrdU+/PH3- nuclei are found on the apical side of the retina.
591

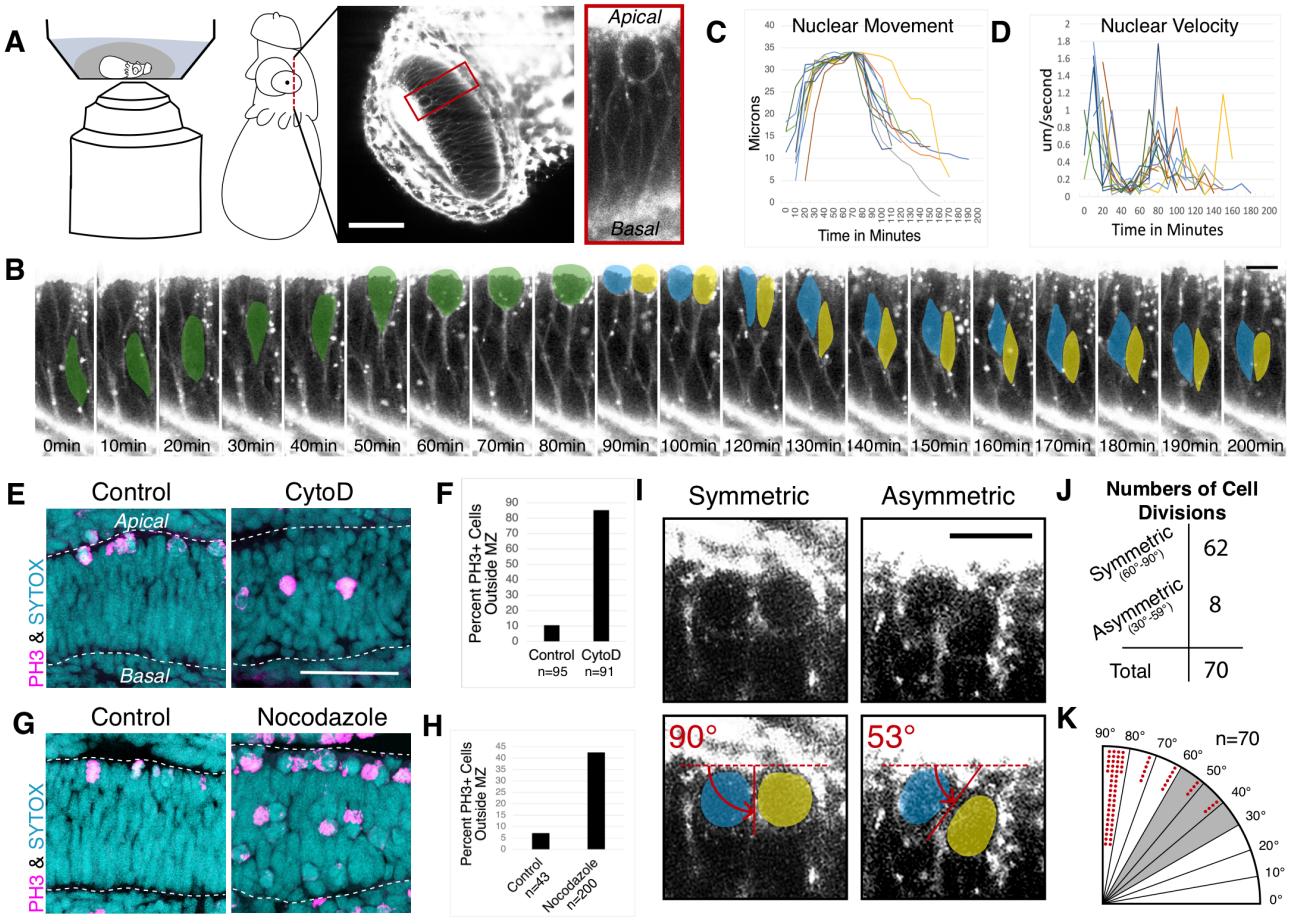

Figure 2: Nuclear migration and mitosis in the retinal epithelium. A. Schematic of squid embryo live-imaging. Scale is 50um **B.** False-colored timelapse of a single mitosis in the squid retina at stage 23 showing apical migration in the epithelium, mitosis, and basal migration. Apical is up, basal is down. Scale is 10um. **C.** Graph of nuclear movement as tracked using the Trackmate Fiji plugin (Schindelin et al., 2012). 13 nuclei tracked in 3 embryos. Tracks aligned to the highest point in migration. **D.** Graph of nuclear velocity calculated from the cells tracked in C. **E.** PH3 immunohistochemistry on actin polymerization inhibited squid retina at stage 23. 5uM Cytochalasin D and DMSO control treatment for 7 hours and immediate fix. Scale is 50um. **F.** Quantification of PH3+ nuclei away from the mitotic zone. **G.** PH3 immunohistochemistry on microtubule polymerization inhibited squid retina at stage 23. 5uM Nocodazole and DMSO control treatment for 7 hours and immediate fix. **H.** Quantification of PH3+ nuclei away from the mitotic zone. **I.** Example of symmetric and asymmetric cell divisions observed in live-imaging experiments. Measurement angle of division shown. Scale is 10um **J.** Quantification of symmetric (60°-90°) and asymmetric (30°-60°) cell divisions quantified from videos of 5 embryos and a total of 70 mitoses. **K.** Radial histogram quantification of division angles.

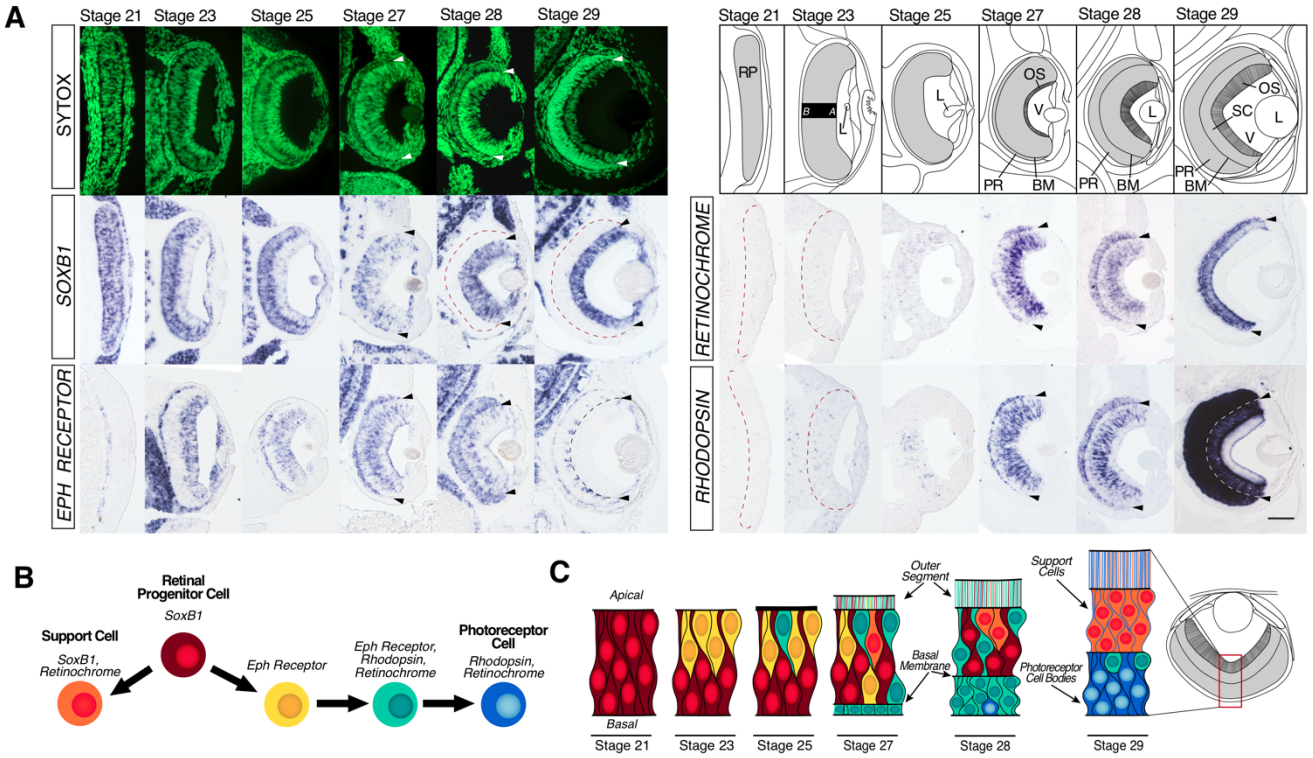

Figure 3: Molecular marker expression suggests a retinal differentiation trajectory. **A.** Staged mRNA expression in the developing cephalopod retina: *DpSoxB1, DpEphR, DpRhodopsin, DpRetinochroome*. Nuclear stain (sytox) shown in green. Arrowheads and the black and white dotted lines identify the basal membrane. Red dotted lines identify the posterior retinal boundary. Scale is 50um. *RP,* Retinal Placode; *L* Lens; *OS,* Outer Segment; *BM,* Basal Membrane; *PR,* Photoreceptor Cells; *V,* Vitreous Space; *A,* Apical; *B,* Basal. Stage 21, 23, & 25 embryo anterior is down. Stage 27, 28, & 29 embryo dorsal is up. **B.** Color key and hypothesis of cell differentiation trajectories. **C.** High magnification summary of time course gene expression data. At stage 21 the retina is homogenous. At stage 23 the retina is divided into apical and basal regions. At stage 25, evidence of terminal differentiation markers, *DpRhodopsin* and *DpRetinochrome*, are evident. At stage 27, the first nuclei are found behind the basal membrane and strict segregation of apical and basal expression is lost. Stage 28, the photoreceptor cell population behind the basal membrane grows and gene expression shows increased regional segregation. Stage 29, differentiation markers are robustly expressed.

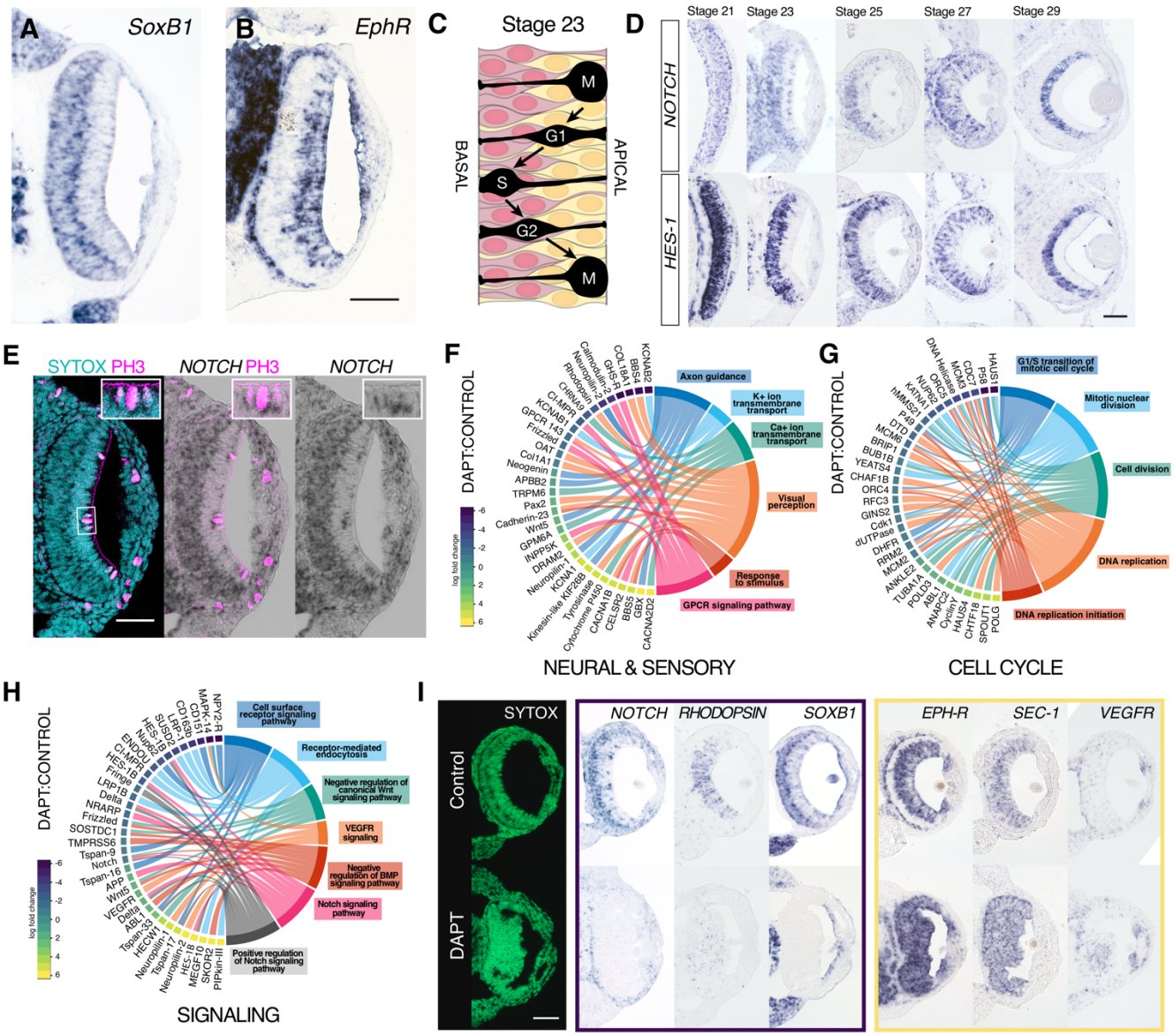

Figure 4: Notch signaling is required to maintain retinal progenitor cell identity. A. *SoxB1* expression in retinal progenitor cells on the basal side of the retina at stage 23. **B.** *EphR* expression in post-mitotic cells on the apical side of the retina at stage 23. Scale 50um. **C.** Schematic of nuclear migration within the pseudostratified retinal epithelium. Red (*DpSoxB1*) and yellow (*DpEphR*) color corresponds to gene expression and summary Figure 3B and 3C. **D.** *DpNotch* and *DpHes1B* expression correlates with *DpSoxB1* expression in the retinal progenitor cell population. Scale 50um **E.** *DpNotch* expression on the apical side of the retinal epithelium correlates with PH3 expression. Scale 50um. **F.** DAVID GO-annotations of RNA-seq results of Notch inhibited eyes. Embryos treated with 20uM DAPT and DMSO control at stage 23 for 24 hours. Eyes dissected for sequencing. All results shown have a p-value < 0.05. Neural sensory genes **G.** Cell-cycle genes **H.** Signaling pathway genes. Color Key is shared for all RNA-seq results. **I.** *In situ* hybridization on Control and Notch inhibited retina. Embryos treated with 20uM DAPT and DMSO control at stage 23 for 24 hours and fixed immediately. Down-regulated genes in DAPT embryos the box on the left. Up-regulated genes in DAPT embryos on the right. *DpSoxB1* expression, the retinal progenitor marker, is lost from the retina in Notch inhibited embryos. *DpEphR* expression, the neuroblast marker, has expanded expression throughout the retina in Notch inhibited embryos.